11

Simulating Alpine Tundra Vegetation Dynamics in Response to Global Warming in China

Yanqing A. Zhang[1], Minghua Song[2], and Jeffery M. Welker[3]
[1]Department of Geography, and School of Computing Science, Simon Fraser University, BC,
[2]Institute of Geographic Sciences and Natural Resources Research, the Chinese Academy of Sciences, Beijing,
[3]Environment and Natural Resources Institute, University of Alaska Anchorage, AK,
[1]Canada
[2]P.R. China
[3]USA

1. Introduction

Global temperatures are increasing due to the effects of greenhouse gases emission. It is projected that climate changes will have profound biological effects, including the changes in species distributions as well as vegetation patterns (Walther et al., 2002; Klanderud & Birks, 2003; Pauli et al., 2003; Tape et al., 2006). Many results from observations and experiments (Parmesan, 1996; Molau & Alatalo, 1998; Parmesan et al., 1999; Welker et al., 2000, 2005; Schimel et al., 2004; Sullivan & Welker, 2005), and simulation studies (Cramer & Leemans, 1991; Harras & Prentice, 2003) have depicted alterations in C and N cycling, trace gas exchanges and shifts in the distribution of vegetation boundary and the mixture of shrubs and grasses.

The Tibetan Plateau covers approximately 2.5 million km^2 with an average altitude of more than 4000 m dominated by alpine tundra (Zheng, 2000). Alpine tundra vegetation is predicted to be one of the most sensitive terrestrial ecosystems to changing climate (Korner, 1992; Grabherr et al., 1994; Chapin et al., 1992, 2000). This type of ecosystem is composed of slow-glowing plants and are dominated by the soils which can be concentrated with high organic matter near surface soil that undergo frost heave and cryoturbation (Billings, 1987; Xia, 1988). Both plant growth and possible organic matter decomposition are predicted to increase under warmer climates, which may cause alpine ecosystem carbon flux and energy flow changes (Chapin et al., 1997; Kato et al., 2006). Simultaneously, warmer weather may increase plant growth, and primary production (Bowman et al., 1993; Wookey et al., 1995) as well as changes in species dominance (Walker et al., 1994; Klein et al., 2007). We report findings that are derived from a short–term responses to simulated environmental warming, focusing on aboveground biomass of three dominated life forms and community compositional attributes.

Based on 38 years (1959-1996) of climate observations and statistical analysis, the annual mean temperature increased during this period ranged from 0.4 to 0.6°C in the area of

Haibei Alpine Tundra Ecosystem Research Station (Li et al., 2004), that is located on north-eastern part of Qinghai-Tibetan Plateau (37°N, 101°E). In order to study alpine tundra vegetation changes at the regional scale, we model alpine tundra vegetation spatial and temporal dynamics in response to global warming by integrating a raster-based cellular automata and a Geographic Information System (Zhang et al., 2008). Temperature changes across the study area are not only due to elevation, but also to aspect and distance from the nearest stream channel. The liner regression model provided a temperature spatial distribution based on elevation alone, which is the primary step. The normalized temperature surface created by the Multi-Criteria Evaluation (MCE) is highly representative of the potential temperature distribution in a normalized fuzzy format. Assuming each vegetation type in the raster cell unit reacts as homogeneous entity, we conduct a spatial and temporal simulation by combining cellular automata and MCE provided in the IDRISI software (Eastman, 2003).

Global changes have strong effects on terrestrial ecosystems but with significant regional differences. The Tibetan Plateau is currently experiencing rapid changes in temperature (Zhang et al., 1993). Fluctuations in temperature have had significant effects on alpine tundra ecosystem, which produces the important changes in the global energy balance and carbon budget (Cao & Woodward, 1998; Zhou, 2001; Kato et al., 2006). The Qinghai-Tibetan Plateau is situated in southwestern China (Fig. 1), and is the highest continental

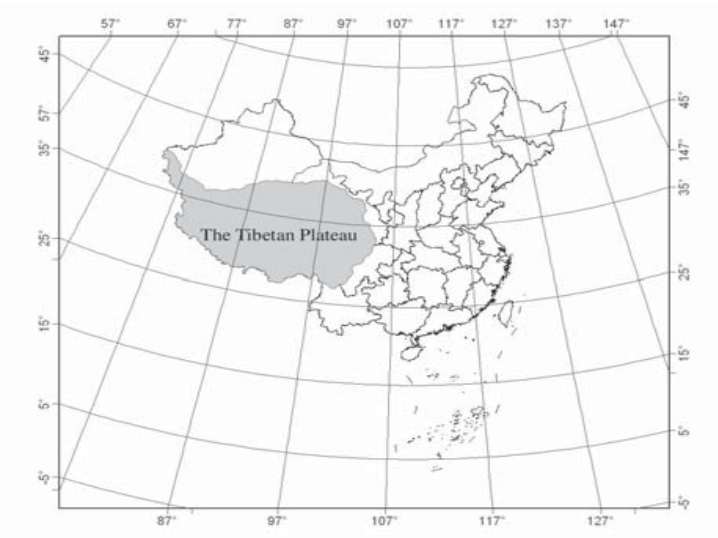

Fig. 1. The location of the Tibetan Plateau in China.

landmass in the world. Elevation ranges from 2500 to 8000 m with an average altitude of more than 4000 m. Uplifting of the plateau created and then strengthened the South Asia Monsoon, and affects terrestrial ecosystems in China owing to its unique location and high elevation (topography) (Zhang, 1993; Thompson et al., 1989). The development and evolution of species and vegetation on the Qinghai-Tibetan Plateau were influenced significantly by a fluctuating climate during the uplift. Ni (2000) simulated biomes on the Tibetan Plateau using the improved BIOME3 model (BIOME3-China) under the present

climate conditions, as well as under a scenario with a CO_2 concentration of 500 ppmv. A combined biogeography biochemistry model, BIOME4 (Kaplan et al., 2003) was improved to simulate the alpine vegetation changes at the biome level (Song, et al., 2005).
In this chapter, we review the important ecological findings from simulated environmental changes on the alpine tundra vegetation (Zhang & Welker, 1996). We present a changing alpine tundra vegetaion using Vegetation Dynamic Simulation Model (VDSM) integrated with scenarios of global temperature increase of 1 to 3°C (Zhang et al., 2008). With BIOME4 model (Song et al., 2005), we illustrate the vegetation biomass changes and the vegetation distribution dynamics in the region of Qinghai-Tibetan Plateau in responses to global warming.

2. Tibetan alpine tundra above ground biomass and community responses to simulated changes in climate

A suite of abiotic conditions may be modified as weather patterns and regional climates change altering biospheric and atmospheric processes in tundra ecosystems (Maxwell, 1992; Shaver et al., 1992; Jonasson et al., 1993; Grabherr et al., 1994; Larigauderie & Korner, 1995). For instance, warmer air temperatures will likely alter the flux of water from these ecosystems to the atmosphere drying soils and contributing to increased cloud formation. Simultaneously, warmer conditions may increase plant growth, primary production and carbon sequestration, so long as cloud cover is not affected and other factors such as water or nutrients do not limit photosynthesis and growth (Haag, 1974; Bowman et al., 1993; Wookey et al., 1995).
The ecological consequences of changes in tundra environmental conditions will be manifested in a host of processesincluding shifts in primary production (Bowman et al., 1993; Walker et al., 1994), trace gas fluxes (Brooks et al., 1995), plant and soil mineral nutrition (Nadelhoffer et al., 1991; Shaver & Chapin 1991), reproductive plant biology (Wookey et al., 1993, 1994), leaf carbon isotope discrimination (Welker et al., 1993), as well as changes in species dominance (Walker et al., 1994). However, it is unclear whether all these processes are sensitive to short-term changes in environmental conditions in all tundra habitats or whether multiple years of climate change are necessary to elicit detectable alterations in plant performance and species abundance. To date, most studies of alpine tundra responses to in situ changes in climate, using field manipulations, have been confined to sites in North America and in Western Europe (Kmrner, 1992; Chapin et al., 1995; Kennedy, 1995) without the consideration of the extensive alpine tundra in Asia, and in particular, western China.

2.1 Experimental treatments and obervations

Our research site is located near Haibei Alpine Meadow Ecosystem Station (37°N, 101°E) at an elevation of 3250 m (Xia, 1989; Cincotta et al., 1992). The vegetation of our friel site is typical of a *Kobresia humilis* meadow (Zhou et al., 1987, Zhang & Zhou, 1992). Our field experiment was initiated in June 1991 and the first season was complated in October 1991. Four treatments were implemented as (1) Minigreenhouses (G) (2) Shade (S) (3) Side Fences (SF) (4) Control plot (C). The size of experimental plot is 2 m x 5 m. A completely randomized design was used to establish the 16 treatment plots consisting of four treatments (G, S, SF, C) replicated four times. The detail site setup, microclimate monitoring and friel observation were described by Zhang and Welker (1996).

The greenhouse treatment increased mean air temperature by 20% from 12.4 to 17.8° Cover the course of the growing season (Table 1). Warmer air temperature subsequently caused higher soil temperatures at 5, 10, and 15 cm under greenhouse (G) as opposed to ambient (C) conditions (Table 1). The mean vapor density was significantly increased under

Treatments		Control	Green-house	Shade	Side fence
Mean air temperature (°C)		12.38	17.78	14.33	12.91
Mean soil temperature (°C)	5 cm	12.79	16.07	13.85	12.44
	10 cm	12.29	15.14	12.76	12.06
	15 cm	12.19	13.95	12.74	12.10
Vapor density (g m^{-3})		4.00	12.00	6.00	5.80
Soil suction (Kpa)	10 cm	14.80	21.07	30.39	14.94

Table 1. Abiotic conditions from the four treatments between July and October 1991

warmer temperatures of the greenhouse (G) from 4 to 12 g m^{-3}. The soil suction was essentially the same between all treatment plots, except for under shaded (S) conditions, and the soil suction was consistently higher indicating a very lower soil water content for a dryer envrimental condition. The shade treatment (S), while reducing irradiance, also resulted in a slight increase in air temperature and soil temperature at 5 cm. The shade treatment (S) had no effect on soil temperatures at 10 cm or 15 cm nor did the shade treatment alter the vapor densities. Side fences (SF) had no effect on ambient air temperatures and subsequently no effect on soil temperatures.

2.2 Results and discussions

Total community aboveground biomass in all four treatments was not significantly different in July (Table 2). The peak aboveground biomass between Greenhouse (G), occurred in September 351.36 g m^{-2}, and ambient (C) condition, occurred in October 346.19 g m^{-2} have no significant difference at Haibei Apline Meadow Ecosystem Research Satation. However, lowered irradiance (S) resulted in a 23% decrease in total community biomass within 5 wk of treatment applications. Total biomass under reduced irradiance (S) continued to be the lowest over the course of the season reaching a maximum of only 80% of the peak biomass under ambient (C) conditions.

Total maximum aboveground biomass at our Tibetan alpine tundra site ranged from 161 to 351 g m^{-2} under ambient conditions (Table 2). These ranges in biomass are similar to the peak aboveground biomass at other alpine tundra sites such as on Niwot Ridge, Colorado, U.S.A., where the intercommunity aboveground biomass in different vegetation types ranges from 71 to 309 g m^{-2} (Walker et al., 1994). Our environmental manipulations simulating climate warming resulted in warmer air and soil temperatures between 1 and 5°C, which is within the ranges of increase reported for higher elevations in Western Europe

over the past 15 years (Rozanski et al., 1992; Grabherr et al., 1994) and is within the ranges predicted for tundra habitats under a doubling of CO_2 over the next 50 yr (Maxwell et al., 1992). The season long average increases are also similar to those accomplished in other tundra experimental warming treatments though our lack of nighttime measurements means our averages are slightly higher than those actually experienced by plants and soil in these treatment plots (Chapin & Shaver, 1985; Wookey et al., 1993; Parsons et al., 1994; Kennedy, 1995). However, most importantly, higher temperatures were maintained in our warmed plots into October and may partially explain the extended growing season observed for grasses.

Date	3 Jul.	1 Aug.	2 Sept.	2 Oct.
Control	161.16 ± 10.23[a]	269.36 ± 17.57[a]	351.36 ± 15.55[a]	285.68 ± 5.49[b]
Greenhouse	157.52 ± 7.13[a]	252.37 ± 16.57[a]	334.61 ± 13.97[a]	346.19 ± 11.81[a]
Shade	145.86 ± 7.51[a]	206.69 ± 17.63[b]	278.93 ± 13.78[b]	266.21 ± 10.63[b]
Side fence	164.00 ± 9.25[a]	247.30 ± 10.80[a]	370.08 ± 6.45[a]	300.80 ± 5.07[b]

Differences between the treatments within each month at $p < 0.05$ are noted by different letters.

Table 2. Total aboverground biomass (g m^{-2}) from the four treatments in July, August, September, and October 1991

Aboveground biomass was initially similar among all treatments for forbs, sedges and grasses (Fig. 2a). Within 5 weeks after the warming treatments were implemented, grass biomass was significantly higher in the warmed as compared to control conditions (Fig. 2b). Conversely, grass biomass was significantly reduced during this same period under shaded conditions (Fig. 2b). Reductions of wind using side fences (SF) had no significant effect on grass, sedge or forb biomass (Fig. 2b). By September, grass biomass differences between control and warmed plots were nonsignificant though forb biomass was significantly ($p < 0.05$) lower in the greenhouses (G) as opposed to control conditions (C) (Fig. 2c). Lower irradiance had a significant effect on grass growth and in September, grass biomass was 36% less in shaded (S) as opposed to control conditions. Forb biomass was slightly higher in side-fenced areas as compared to control conditions. Between September and October grass in control plots started to senesce and biomass began to decline (Fig. 2c, 1d). However, under warmed (G) conditions, grass biomass was significantly ($p < 0.01$) higher in warmed as opposed to control conditions in October which postponed community senescence (Fig. 2d). This prolonged growth, or postponed senescence during the fall in warmed plots occurred as the greenhouses maintained warmer air and soil temperatures than ambient conditions. Biomass of grasses and forbs were slightly lower under shaded (S) conditions in October, while sedge biomass was significantly ($p < 0.05$) higher under these same reduced irradiance conditions (Fig. 2d).

Species importance values as a measure of community level responses are presented in Table 3. Under reduced radiation (S) reductions in *Elymus* and *Festuca* were associated with increases in *Stipa* and *Scirpus* which dramatically altered the composition and structure of these plant communities. Changes in community composition and structure under warmer conditions (G) were manifested by lower importance values for *Poa* and *Kobresia* with corresponding increases in importance values for *Stipa* and *Oxytropis* (Table 3).

Grass and forb biomass production was especially sensitive to warmer conditions (Fig. 2). Grass aboveground biomass was 25% greater under warmer conditions after only 5 week of warming while forb biomass decreased by 30% (Fig. 2b). Differences in aboveground grass

biomass between warmer and control conditions were diminished by September when grass biomasses were not significantly different (Fig. 2c).

However, it appears that community senescence, which usually starts in September, was postponed until sometime in October under warmer (G) conditions as evidenced by no decline in aboveground community biomass between September and October (Table 2). This postponing of senescence and subsequently an extension of the growing season under warmed conditions, resulted in part because peak grass biomass was not realized until early October amounting to 177 g m-2 (Fig. 2d). The ability of the grass life form at our site to exhibit a rapid, positive response to warmer conditions and to extend the season of growth is likely the result of (1) the existence of a large leaf area at the time of treatment application, (2) the inherent physiological capacity of grasses to alter patterns of resource allocation (Welker et al., 1985, 1987; Welker & Briske, 1992), (3) their morphological and demographic capacity to elongate fall tillers (Briske & Butler, 1989), and (4) the ability to grow when environmental constraints are temporally removed (Sala et al., 1992). Grasses at other tundra sites have also exhibited an ability to respond rapidly to simulated changes in climate as exemplified by *Calamagrostis* biomass increases in the sub-arctic at Abisko, Sweden under warmer conditions (Parsons et al., 1995). The grass growth response reported by Parsons et al. (1995), in what is typically a dwarf shrub dominated ecosystem, was due in large part to

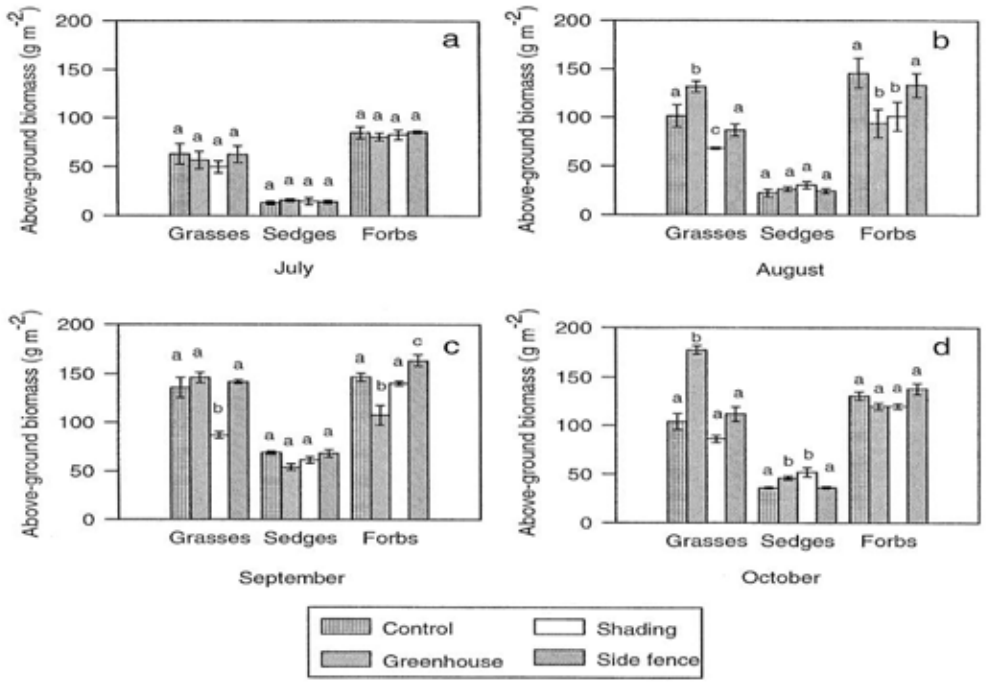

Fig. 2. The aboveground biomass of grasses, sedges, and forbs in control, greenhouses, shaded, and side fenced treatment plots sampled in July, August, September, and October 1991. Superscripts of the different letters denote biomasses which were significantly different ($p < 0.05$) for each individual sampling date.

Plant species	C	G	S	SF
Elymus nutans	52.05	54.07	23.80	56.09
Festuca ovina	35.05	39.08	23.64	33.42
Poa pratensis	21.12	14.53	27.99	20.04
Koeleria cristata	26.32	17.63	18.22	23.86
Stipa aliena	22.29	29.01	31.74	21.21
Kobresia humilis	19.65	6.55	18.66	23.85
Carex scabriostris	12.62	10.14	14.04	13.32
Scirpus distigmaticus	15.10	10.72	35.22	16.54
Saussurea superba	24.16	30.61	27.18	21.13
Gentiana aristata	8.15	10.11	22.13	10.01
Oxytropis ochrocephala	16.17	34.95	15.82	26.33
Trigonella ruthenica	8.69	16.33	8.01	7.75
Taraxacum mongolicum	8.67	10.93	9.48	9.19
Potentilla bifurca	10.50	10.20	9.02	13.94
Aster flaccidus	15.34	9.25	8.62	5.71
Oxytropis caerulea	11.87	13.55	11.23	8.40
Potentilla anserina	8.83	8.74	8.67	16.91
Gentiana straminea	14.65	8.86	21.62	14.88

[a] C—control; G—greenhouse; S—shade; SF—side fence.

Table 3. The Important value of domiant plant species between four treatment plots[a]

an extensive, preexisting network of underground *Calamagrostis* meristems, capable of rapid shoot extension and leaf development up through the dwarf shrub understory.

The shift in alpine tundra community biomass characteristics whereby maximum biomass is maintained into the autumn is different from what might be observed in arctic tundra dominated by deciduous dwarf shrubs. Prolonged growth of many arctic plants in autumn is unlikely due to photoperiodic cues which control senescence (Murry & Miller, 1982). Thus, even if conditions in arctic tundra were warmer in fall, the ability of many dominant life forms to either produce new fall foliage or continue expansion of existing leaf and shoot biomass is limited by life history traits. And while graminoids, such as *Eriophorum* may constitute a large fraction of the biomass in these systems (Shaver et al., 1992), extended growth in fall under warmer temperatures may be unlikely due to the low solar angles in autumn.

The ability of grasses to utilize favorable conditions at the end of the season is a trait similar to that observed for other tundra lifeforms such as evergreen shrub species (Karlsson, 1985; Welker et al., 1995). For instance, Welker et al. (1995) have found evidence that *Dryas octopetala*, a wintergreen species, has the capacity to exhibit net carbon assimilation at the end of the season under warmer, wetter, and fertilized conditions when plants in control conditions have ceased gaining carbon, which is made possible in part by its evergreen nature. In addition, Karlsson (1985) found that 20% of the carbon acquired by the evergreen dwarf shrub, *Vaccinium vitisidaea* occurred in spring and in autumn, before leaf emergence or after leaf senescence in the deciduous species, *Vaccinium uliginosum*. Thus, evergreen dwarf shrubs are also a tundra life form which due to their inherent life history characteristics can respond to changes in environmental conditions which occur in spring, and fall (Wookey et al., 1993; Welker et al., 1995).

The opportunistic behavior of grasses we observed was not evident for forbs. During the initial 5 weeks, forb biomass was reduced under warmer conditions while grass biomass was increasing (Fig. 2b). The opposite response for forbs may have been due in part to the grasses out-competing forbs for water, nutrients and or light. However, the overall community level response was that total biomass was not different between warmed (G) and control (C) conditions after 5 weeks of experimental applications (Table 2). This observation of similar community biomass under modified environmental conditions is consistent with the observations of Chapin and Shaver (1985). These authors found that arctic tundra total community production (current years growth) in perturbed and in control plots remained the same. This inherent buffering was achieved because some species or life forms increased growth while others exhibited reduced growth. They concluded that conditions favorable for one species or life form are less favorable for others, though the total community or ecosystem production changes annually very little (Chapin et al., 1995). This attribute of tundra ecosystems may be the result of the inherently low nutrient levels available to plants in tundra which constrains system level primary production (Shaver et al., 1992).

The one life form in our study which appeared to be the least responsive to simulated climate warming were the sedges, consisting primarily of Kobresia humillis. The lack of significant increases in biomass until the end of the first season under warmer or shaded conditions indicates that this life form has a relatively low sensitivity to temperature and irradiance. However, other sedges, such as Kobresia myosuroides on Niwot Ridge, Colorado, exhibits an increase in biomass under elevated nutrient availability (Bowman et al., 1993). This would suggest that while the warmer conditions in soils under our minigreenhouses may have elevated soil mineralization and increased nutrient pools available to plants (Jonasson et al., 1993; Robinson et al., 1995) the increases were either not sufficient to alter Kobresia growth, or that Kobresia root uptake rates are low, and its ability to compete for soil nutrients with grasses is low (Black et al., 1994; Falkengren-Grerup, 1995). Even though soil nutritionm may have been altered under warmed conditions, the ability of sedges at our site to acquire these resources in a competitive setting appears to be limited, in part due possibly to resource capture by soil microbes (Jackson et al., 1989). However, in future years changes in rooting patterns may enable this species to capitalize on changes in soil resources.

In conclusion, our findings suggest that Tibetan alpine grasses are predisposed to rapid increases in biomass under simulated climate warming due in part to their inherent life historytraits. In addition, the ability of grasses to produce tillers late in the season under warmer conditions extends the period of carbon gain and extends the period in which the community exhibits maximum aboveground biomass. We find that sedges at our site are insensitive in the short term to changes in environmental conditions, while forbs may decrease at the expense of grass biomass. Increases in cloudiness over the Tibetan alpine tundra would likely result in lower aboveground biomass, but if accompanied by higher rainfall the effects may be counter-acting. The extension of peak community biomass into the autumn may in the long term have cascading effects on net ecosystem CO_2 fluxes, nutrient cycling, and forage availability to grazers (Welker et al., 2004).

3. Cellular automata: simulating alpine tundra vegetation dynamics in response to global warming

Spatial modeling processes are available in current GIS software such as IDRISI, which is capable of dealing with a large set of raster data and manipulating the data via operations in

a series of discrete time steps, where single raster cells can be influenced by their neighborhood or other data in an overlay. All map layers are imposed on the same grid system. This type of GIS environment provides a sophisticated tool to help us target the real problem in a complex system (Wolfram, 1984; Coulelis, 1985; Itami, 1994; White & Engelen, 2000; Giles, 2002). In our study, we use GIS analysis, linear regression, MCE, cellular automata (CA), and a raster image calculator to build a unique Vegetation Dynamic Simulation Model (VDSM). Global warming scenarios are interpreted as inputs of the spatial parameters. Large processing tasks are completed by the computer system.

The predicted outcome of this study is that individual vegetation types will respond to a global mean temperature increase (GMTI) in 2100 of 1 or 3°C by either expanding or shrinking their range because of plant species' suitability to the warmer and drier climate conditions. This corresponds to 0.1 or 0.3°C per decade, respectively (Johnes & Briffa, 1992; Leemans, 2004).

3.1 Methods and simulation model

3.1.1 Data set

Our study area is located near the Haibei Alpine Meadow Ecosystem Resaerch Station, Qinghai Province, China (37°29'-37°45'N, 101°12'-101°33'E) (Zhang & Zhou, 1992). The elevation in the study area varies from 3000 to 4500 m a.s.l. The model uses the following data:

- A 90 m x 90 m resolution DEM;
- Temperature derived from the DEM using an empirical linear regression model (Zhang, 2005);
- Land surface parameters (aspect, slope, stream channel density) derived from the DEM using GIS analysis tool provided in the IDRISI software (Eastman, 2003);
- A raster vegetation map (30 m x 30 m pixels) produced in 1988 (Zhang, 2005). The vegetation map with a total of 10 vegetation classes is resampled to match the DEM resolution (90 m x 90 m) (Fig. 3).

3.1.2 Multi-criteria evaluation

Constrains are defined as the limited area that are not considered to be natural vegetation, such as water bodies, glaciers, gravel slpoes and artificial grasslands. They represent area where the natural vegetaion cannot grow or are otherwise constrained. A Boolean image is created to display inclusion and exclusion of the constraint conditions.

$$y = MCE\ (F\ 1, F\ 2, F\ 3, ...Fn) \quad (1)$$

The factors (F1, F2, .…Fn) used in the MCE are selected based on the most important variables that determine the output y in Equation (1).

We use MCE in step 1 (Fig. 4) to determine a normalized surface temperature, which calibrates the temperature by these spatial parameters: aspect, suitable surface temperature, and distance to the nearest stream channel.

The temperature varies along with these spatial parameters: (1) It increases from the north (a=0°) to the southeast (b=145°), with the highest values from the southeast to the southwest (c =275°), then decreasing to the north (d =360). The change pattern can be described as a sigmoidal fuzzy function type, in a symmetric shape with specific values (a, b, c, d) in Table 4. (2) In the lower valley of our study area, the monthly mean temperature in July is 10.1°C

(Li et al., 2004). The temperature decreases with increasing elevation. We define the temperature less than a=0°C as unsuitable for alpine plant growth. The temperature from 0°C to b=5°C is defined as less suitable for alpine plant growth; the temperature from 5°C to c=13°C is defined as most suitable. The temperature from 15.5°C to d=18°C reduces the

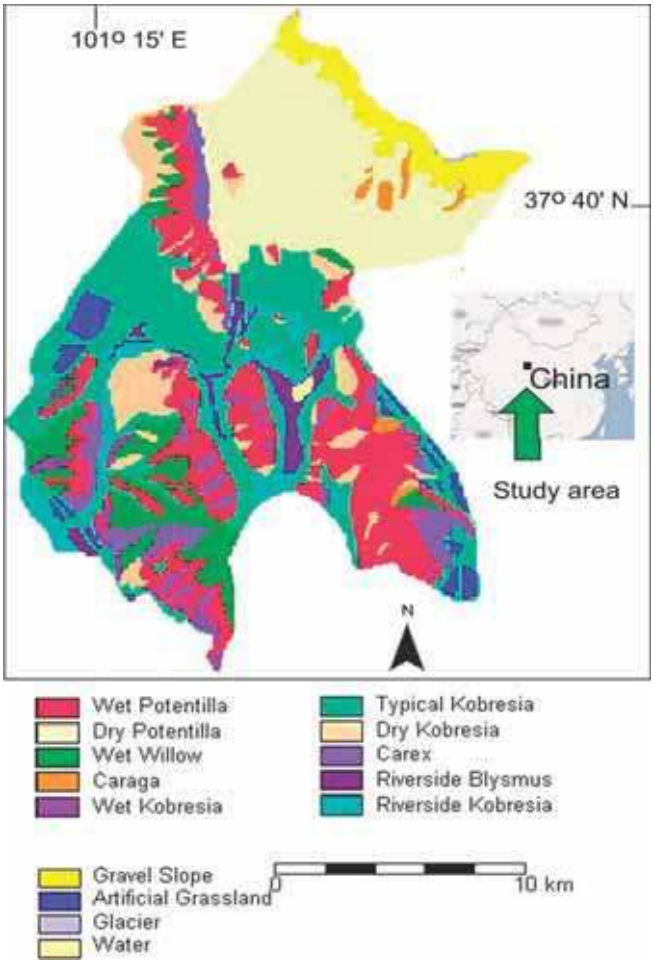

Fig. 3. Haibei Alpine Tundra Vegetation Distribution, 1988

suitability for alpine plant growth, representing the dry, south-facing areas (Table 4). In the Analytical Hierarchy Process (AHP), the most important temperature is in the range of b=5°C to c=13°C, which present the sigmoidal fuzzy function type and symmetrical shape. (3) The distance to a stream affects the temperature. If the area is within 10 m of a stream or water body, its temperature is closer to the stream or water temperature; beyond 600 m from a stream or water body, the temperature is minimally affected by the nearest water bodies. The values are defined as a = 10 m, b = 600 m, with a sigmoidal fuzzy function type and monotonically deceasing shape.

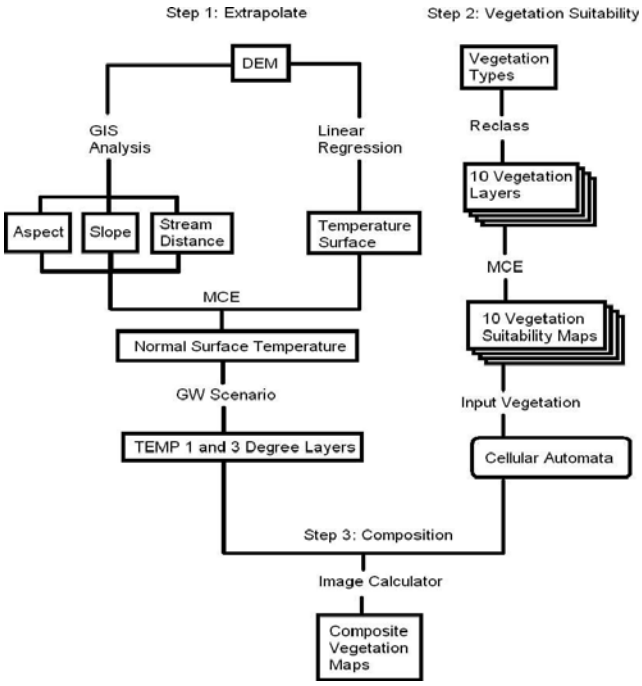

Fig. 4. Vegetation Dynamic Simulation Model (VDSM)

	Factors to standardize with fuzzy	Membership function type	Membership function shape	a	b	c	d	AHP weights
Temperature	aspect	Sigmoidal	Symmetric	0	145	275	360	0.2631
	temperature suitability	Sigmoidal	Symmetric	−2	5	13	16	0.5472
	distance to stream	Sigmoidal	Monotonically decreasing	10	600	—	—	0.1897

Notes: aspect: 0–360°; temperature suitability: oC; distance to stream: meters; a, b, c, d: suitabilities for the factors; AHP weights derived from pairwise comparison up to an acceptable level.

Table 4. Normalized surface temperature's fuzzy membeship function types and shapes, factor's suitability values (a,b,c,d) and AHP weights

In step 2 (Fig. 4), we use the MCE method and create a suitability map for each vegetation type using the aspect, slope, and the distance to stream channels. The suitability values (a, b, c, d) in Table 5 are defined based on the vegetation distribution in the study area (Zhang & Zhou, 1992). The fuzzy membership function type and shape and AHP weights for each vegetation are calculated and reported in Table 5 (Eastman, 2003).

3.1.3 Macro modeler

The macro model is created to simulate changes in each vegetation type through time and space, integrating operations such as overlay, scalar, fuzzy module, and cellatom (Fig. 5). These operations are available in the IDRISI software package (Eastman, 2003) and have to be built in Macro Modeler with an initial scalar value (0.0–1.0) and fuzzy set values (0–255). The GMTI scenarios are implemented in the Macro Modeler by adjusting the scalar operation to increase the temperature by 0.1°C in a discrete time period. The same logic is

applicable to 0.3°C in a discrete time period (Leemans, 2004). Running the simulation for 10 iterations, the effects of increasing temperature on each vegetation type are accumulated in the output image.

Vegetation type	Factors to standardize with fuzzy	Membership function type	Membership function shape	a	b	c	d	AHP weights
Wet Potentilla	aspect	Sigmoidal	Monotonically decreasing	0	3	—	—	0.1842
Shrub	Slope	Sigmoidal	Symmetric	0	10	20	40	0.2118
	distance to stream	Sigmoidal	Symmetric	0	1500	2000	3700	0.184
Dry Potentilla	aspect	Sigmoidal	Symmetric	0	180	240	360	0.2627
Shrub	Slope	Sigmoidal	Monotonically Increasing	0	25	—	—	0.1595
	distance to stream	Sigmoidal	Monotonically Increasing	0	1800	—	—	0.1782
Wet Willow Shrub	aspect	Sigmoidal	Symmetric	0	225	300	360	0.4434
	slope	Sigmoidal	Symmetric	0	12	22	40	0.1874
	distance to stream	Sigmoidal	Symmetric	0	500	2000	3700	0.3692
Cataplus Shrub	aspect	Sigmoidal	Symmetric	0	240	300	360	0.4934
	slope	Sigmoidal	Symmetric	0	8	12	20	0.1877
	distance to stream	Sigmoidal	Symmetric	0	500	800	3000	0.3487
Wet Kobresia	aspect	Sigmoidal	Symmetric	0	240	300	360	0.825
Meadow	slope	Sigmoidal	Symmetric	0	10	18	30	0.2585
	distance to stream	Sigmoidal	Monotonically decreasing	—	—	200	800	0.1267
Typical Kobresia	DEM	Sigmoidal	Monotonically decreasing	—	—	3500	3800	0.2598
Meadow	slope	J-shape	Monotonically decreasing	—	—	3	10	0.3373
	distance to stream	Sigmoidal	Symmetric	0	50	2000	3000	0.4126
Dry Kobresia	aspect	Sigmoidal	Symmetric	0	200	270	360	0.3956
Meadow	slope	Sigmoidal	Symmetric	0	1	8	18	0.2493
	distance to stream	Sigmoidal	Symmetric	0	200	2200	3800	0.3371
Carex Meadow	aspect	Sigmoidal	Symmetric	0	70	120	200	0.4854
	slope	Sigmoidal	Symmetric	0	10	15	30	0.3108
	distance to stream	Sigmoidal	Symmetric	0	500	900	3500	0.1918
Riverside Blysmus	DEM	Sigmoidal	Monotonically decreasing	—	—	3200	3300	0.6483
Meadow	slope	Sigmoidal	Monotonically decreasing	—	—	9	30	0.2297
	distance to stream	Sigmoidal	Monotonically decreasing	—	—	0	800	0.122
Riverside Kobresia	DEM	Sigmoidal	Monotonically decreasing	—	—	3200	3300	0.3398
Meadow	slope	Sigmoidal	Monotonically decreasing	—	—	9	30	0.287
	distance to stream	Sigmoidal	Monotonically decreasing	—	—	0	800	0.1634

Note: Slope:0-90°; DEM: indicates elevation range for relatively flat area; for others, refers to the note on Table 4

Table 5. Ten vegetation types' Fuzzy membership function types and shape, factor's suitability values (a,b,c, and d), and AHP weights

The cellular automata module is implemented in the Macro Modeler (Fig. 5) and used to form a uniform raster image to represent global warming effects in a spatial context, which operates over discrete time steps (Coulelis, 1985; Giles, 2002; White & Engelen, 2000). The change in each cell depends on the parameters or requirements set by the user and the surrounding neighbors (Wolfram, 1984; Itami, 1994; Ruxton & Saravia, 1998). This project used the CELLATOM module with a 3*3 filter and reclassifies an output cell if at least 3 neighbors contain non- null values. We define the 10 iterations using the DynaLink module (Eastman, 2003). Winthin each iteration, each vegetation map is dynamically updated by running Cellatom, then it is overlaid with the vegetation suitability map altered by a GMTI of 0.1 or 0.3°C. Thus, after 10 iterations, a final suitable vegetation map is produced. The same dynamic processing is repeated for each vegetation type resulting in a total of 10 vegetation suitability maps in response to warmer weather.

3.1.4 Composite final vegetation map

Our objective is to create a composite vegetation map for each global warming scenario, GMTI of 1 or 3°C over time (Fig. 4). All of the 10 vegetation suitability maps with a GMTI of 1 or 3°C are combined in order to produce a composite map using the image calculator module in IDRISI (Eastman, 2003). The highest suitability among the vegetation types is selected to represent the successful vegetation type in that cell.

$$Veg\_dominant = MAX(Veg1, Veg2, ...Veg10) \quad (2)$$

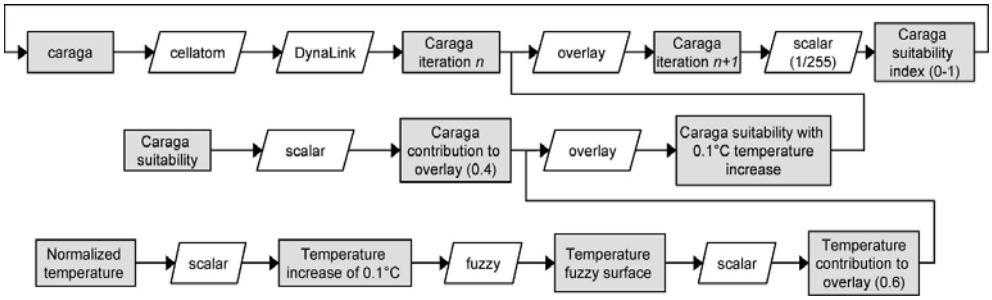

Fig. 5. Example of Macro Modeler incorporating Cellular Automata for Caragana Shrub

Equation (2) above creates a map where the value at each pixel corresponds to the vegetation type with the highest probability of thriving, where Veg1, Veg2 … Veg10 correspond to each of the 10 vegetation types. The 10 resulting maps of dominant vegetation types are overlaid to produce a composite distribution of the most probable vegetation types.

3.2 Results and discussions

3.2.1 Normalized temperature spatial distribution

Temperature changes across the study area are not only due to elevation, but also due to aspect and distance from the nearest stream channel. The linear regression model provided a temperature spatial distribution based on elevation alone, which is our primary step. Furthermore, the normalized temperature surface created by the MCE is highly representative of the potential temperature distribution in a normalized fuzzy format (Fig. 6).

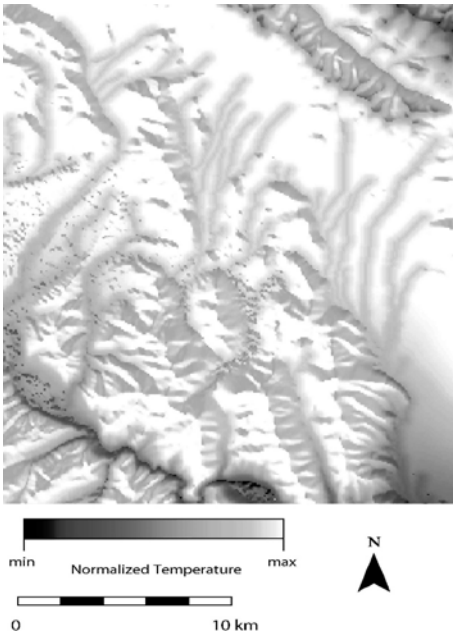

Fig. 6. Normalized temperature with values from 0 to 255.

Temperature distribution is correlated with and controlled primarily by elevation. Numerous spatial interpretation methods have been applied to estimate the spatial distribution of temperature (Li, 2005). The interpolation results do not always agree with the actual sample points, including using geo-statistical methods, and spatio-temporal spline. These methods are highly dependent on the distance to the sample points, and the surface equation. In our study, our first step is to create the primary temperature surface based a linear relation with elevation. The objective is to obtain a more accurate temperature map in terms of aspect, suitable temperature, and distance to the stream. We use the Multi-Criteria Evaluation with Weighted Linear Combination (MCE_WLC) to calibrate the spatial temperature distribution. The fuzzy memberships between the temperature and each factor (aspect, suitable temperature, distance to stream) are based on previous research works (Zhang & Zhou, 1992; Zhang & Welker, 1996; Zhang, 2005). The output, the normalized temperature surface is set into fuzzy format (0–255). Since the temperature is major factor on determining vegetation composition, structure, and distribution, the normalized temperature surface plays an important role when we simulate vegetation dynamics in spatial and temporal dimensions.

3.2.2 Vegetation change comparison

We calculate the percent area change for each vegetation type (Fig. 7) before we compose the final vegetation map. By increasing the global mean temperature (0.1 or 0.3°C per decade), the percent area change of each vegetation type indicates the potential expansion from their original ranges. For example, without competing with other types of vegetation, both Dry *Potentilla* Shrub and Dry *Kobresia* Meadow could expand their vegetation area by 23%. The difference between them is that Dry *Potentilla* Shrub responds more positively to a GMTI of 1°C, and Dry *Kobresia* Meadow responds more positively to a GMTI of 3°C. Similar phenomena are also observed in other vegetation types.

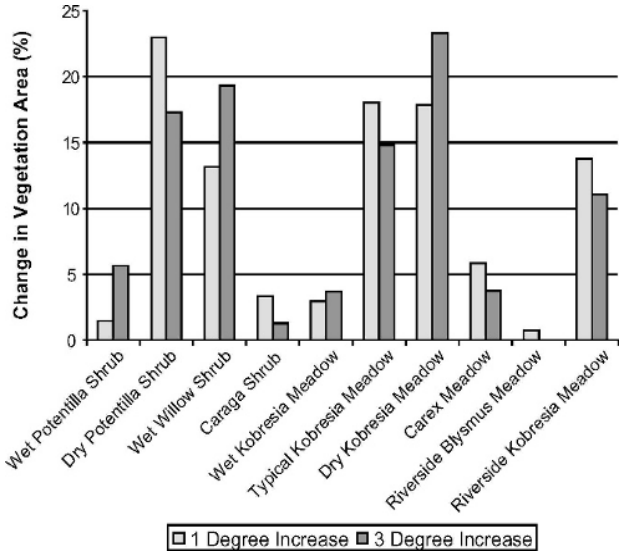

Fig. 7. Percent change in vegetation area with GMTI at 1 and 3°C.

After we compose the final vegetation map, the highest suitability among the vegetation types is finally selected to represent the successful vegetation type in every cell. For instance, Dry *Potentilla* shrub and Dry *Kobresia* meadow expand into areas previously occupied by wet types of vegetation (Fig. 8). The Riverside *Blysmus* meadow, which requires moist conditions, disappears completely with a 3°C temperature increase. In general, the dry vegetation types demonstrate significant expansion from their original ranges and tend to become more dominant in the study area.

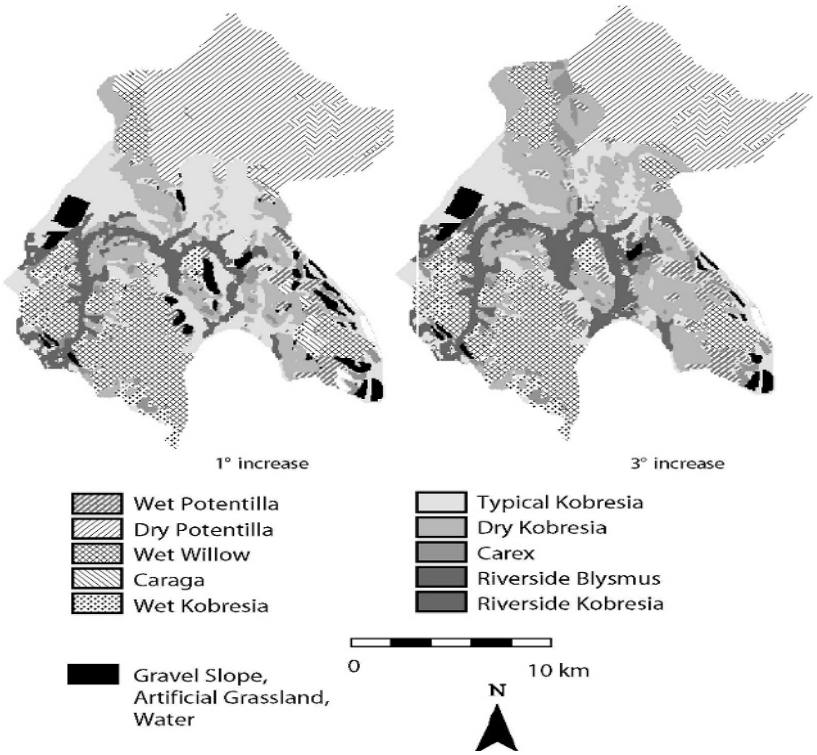

Fig. 8. Final Composite Vegetation Maps For GTMI at 1 and 3°C

3.2.3 Vegetation dynamics over time

The time dimension in the CA module of IDRISI is interpreted as a discrete time step, which corresponds to a temperature-time dimension. The CA module is integrated into the macro modeler, and uses the DynaLink module (Eastman, 2003) to simulate vegetation change within each iteration. The GMTI is defined as a spatial parameter in the deterministic model with a temperature increase of 0.1 or 0.3°C per decade.

3.2.4 Vegetation Dynamic Simulation Model (VDMS)

The VDSM is an example showing that spatial modeling can solve complex ecosystem problems in terms of having the capability to simulate spatial and temporal vegetation dynamics. In this case study, we model the spatial distribution of temperature and create

GMTI scenarios as a spatial grid image. The vegetation dynamics are simulated in discrete time by applying CA in a Macro Modeler. In future studies, this model will be capable of modeling the water-time dimension that makes the simulation more adaptable to global warming research. The VDSM could be potentially incorporated with a normal climate change model to assist in a long-term ecosystem simulation. Alternatively, the VDSM is capable of linking with a stochastic model of temperature change, in which we might be able to forecast an ecosystem disaster.

The VDSM starts by evaluating how to solve a complex vegetation dynamics problem using CA. The VDSM is built by combining the MCE, Macro Modeler, CA, image calculator, Scalar, and Fuzzy functions in IDRISI. Making a clear objective helps us to look into many available modelers and functions in order to solve the problem within the IDRISI software environment. For instance, using Decision Wizard, we create an objective and define a set of constraints, which eliminates the areas that are not natural vegetation. The spatial patterns of the factors (temperature, aspect, slope, and distance to stream) are created as continuous surfaces using Fuzzy functions. The transition rules in Macro Modeler are defined as the maximum potential suitable vegetation in each cell as well as over the study area. The frame work of VDSM (Fig. 4.) is a summary of the model structure and functionalities. VDSM is flexible enough to be integrated with other sub-models that are available from GIScience technology. Figure 3 provides an example of Macro Modeler incorporating Cellular Automata for the modeling of *Caragana* Shrub. In the case of a GMTI of 0.1°C, the suitability map for *Caragana* is weighted at 0.4 and the normalized temperature map is weighted at 0.6. These two factors are combined using the overlay module to produce a map of suitability for *Caragana* Shrub with an incremental temperature increase of 0.1°C. Ten iterations on one vegetation layer are simulated and updated after each iteration using the Cellatom and Dynalink modules. At the end of the iterations, we obtained an accumulated effect of GMTI of 1°C on the vegetation layer.

It would also be possible to incorporate the water layer with the vegetation layer and temperature layer, which can be linked by its weighted value in the VDSM. Thus, the VDSM not only provides a discrete time representation, but also demonstrates how we could develop our model for use with more complex scenarios (Chapin et al., 2006; McGuire et al., 2006).

Compositing a final vegetation map demonstrates the power of GIS analysis in IDRISI. The image calculator module in IDRISI successfully carries out interpolation of the image calculation presented in Equation (2) at the grid cell level. The VDSM illustrates how we could study vegetation dynamics and model many other spatio-temporal phenomena.

The VDSM integrates the suitability maps created from MCE, Macro-Modeler, CA, and spatial environmental factors. And the temperature-time dimension model is incorporated into the VDSM, which makes the temperature a spatial parameter that affects the vegetation dynamics over a discrete time step. The simulating processes conducted by Macao Modeler generate the temperature increase of 0.1 to 0.3°C per decade, which represents the influences of the different global warming scenarios. The results from Fig. 7 and 7 demonstrate that global temperature increase reduces moisture availability (Zhang & Welker, 1996) such that dry vegetation can invade areas previously occupied by vegetation adapted to moist conditions. The structure of the model is generally applicable to other situations, but the particular factors and constraints used in this model are unique to the Haibei alpine tundra ecosystem.

Global warming has strong effects on the alpine ecosystems in terms of altering the biomes and ecosystem biodiversity (Cao & Woodward, 1998; Ni, 2000; Song et al., 2005, Chapin et al., 2006). The alpine ecosystem in the region of the Qinghai-Tibetan plateau is sensitive and

vulnerable to the changing climate (Zhang & Welker, 1996; Kato et al., 2006). The VDSM illustrates that altering global mean temperature changes the alpine vegetation dynamics in terms of having the capability to simulate spatial and temporal vegetation dynamics (Itami, 1994; Leemans, 2004). With the future integration of water condition (Sala et al., 1992; Hodkinson et al., 1999) and disturbance regimes (Zhang, 1990; Cincotta et al., 1992; Zhang & Liu, 2003; Chapin et al., 2006) into the VDSM, the simulation could model more detailed mechanisms and complex feedbacks (McGuire, 2006) of the alpine tundra ecosystem to the changing climate.

4. Simulating Tibetan Plateau alpine vegetation distribution in response to global warming

Vegetation patterns on the plateau were very sensitive and vulnerable to global change, where the growth and distribution of plants depended heavily on local climate conditions (Hou et al., 1982; Zhang et al., 1996). The undisturbed vegetation on the Tibetan Plateau provides an ideal natural laboratory for the research on the sensitivity and responses of alpine vegetation to climate changes. The distributions of the major dominant species and of the vegetation types on the Tibetan Plateau have been investigated since the early 1950s (Anon., 1985). Based on previous research, Zheng (1996) depicted the physiography of the Tibetan Plateau. Ni (2000) simulated biomes on the Tibetan Plateau using the improved BIOME3 model (BIOME3-China) under the present climate conditions, as well as under a scenario with a CO_2 concentration of 500 ppmv. The BIOME3-China used nine plant functional types (PFTs); it did not include the PFTs especially occurring in alpine vegetation, such as cold graminoid or forb, and cushion forb.

In this study, a combined biogeography biochemistry model, BIOME4 (Kaplan et al., 2003) was improved to simulate alpine vegetation at the biome level. We apply the model to the present day, and the end of the 21st century in a scenario with unchecked increase in atmospheric CO_2 concentra tion. We compare the modelled present vegetation to a map of present-day natural vegetation distribution. The future scenario allows us then to assess the sensitivity of alpine vegetation to changes in atmospheric CO_2 concentration and climate.

4.1 Methods

4.1.1 Model description

BIOME4, developed from the BIOME3 model (Haxeltine & Prentice, 1996), is a intergrated carbon and water flux model that predicts the global steady state of vegetation distribution, structure, and biogeochemistry, taking account of interactions among these aspects. The BIOME4 model followed most of the algorithms and rules of BIOME3. It is driven by long-term averages of monthly mean temperature, sunshine and precipitation. In addition, the model requires information on soil texture and soil depth in order to determine water holding capacity and percolation rates. CO_2 concentration is specified. For BIOME4, the improved model using 12 plant functional types (PFTs) that represent broad, physiologically distinct classes, ranging from alpine vegetation (e.g. cushion forbs) to tropical rain forest trees. The PFTs are tropical broad-leaved evergreen, tropical broad-leaved rain-green, temperate broad-leaved evergreen, temperate broad-leaved summergreen, temperate coniferous evergreen, boreal coniferous evergreen, temperate summergreen conifer, temperate grass, temperate xerophytic shrub, cold shrub, cold graminoid or forb, and

cushion forb (Ni, 2000; Kaplan et al., 2003; Yu, 1999). Each PFT is assigned a small number of bioclimatic limits which determine whether it could be present in a given grid cell (Table 6).

Plant Functional Types	Min Tc	max GDD	Min GDD_0	min Tw	max	α min	D
Tropical broad-leaved evergreen	16					0.85	1
Tropical broad-leaved raingreen	12	16				0.80	1
Temperate broad-leaved evergreen	7	12				0.70	2
Temperate broad-leaved summergreen	3	7	1500			0.65	3
Temperate coniferous-leaf evergreen	– 0	3	1200			0.60	3
Temperate summergreen conifer	– 5	7	1200			0.60	3
Boreal coniferous-leaf evergreen	– 8	0	350			0.75	3
Temperate xerophytic shrub	– 2	2				0.30	4
Cold shrub	– 8	– 1	1000	7	11	0.25	5
Temperate grass	– 2	1	1800			0.25	6
Cold graminoid or forb		– 13		5	7	0.40	7
Cushion forb			100			0.45	7

Table 6. Bioclimatic limits of each plant functional type in the model (Tc stands for mean temperature of the coldest month, Tw for mean temperature of the warmest month, GDD for growing degree-days on 5°C base, GDD0 for growing degree-days on 0°C base, α for Priestley-Taylor coefficient of annual moisture availability and D for dominance class).

The computational core of BIOME4 is a coupled carbon and water flux scheme, which determines the seasonal maximum leaf area index (LAI) and maximizes NPP for any given PFT, based on a daily time step simulation of soil water balance and monthly process-based calculations of canopy conductance, photosynthesis, respiration and phenological state (Haxeltine & Prentice, 1996). To identify the biome for a given grid cell, the model ranks the tree and non-tree PFTs that were calculated for that grid cell. The ranking is defined according to a set of rules based on the computed biogeochemical variables, which include NPP, LAI, and mean annual soil moisture. The resulting ranked combinations of PFTs lead to an assignment to one of the biomes (Table 7).

4.2 Climate scenarios

4.2.1 Modern climate data

A Chinese grid-based long-term mean climatology (temperature, precipitation and sunshine) database (1961-1990) was used for a modern vegetation simulation, and as a baseline for other modeling experiments. The climate data for China simulated by the PRISM climate model (Parameter-elevation Regressions on Independent Slopes Model) developed by the Oregon Space Climate Research Center. Daly (1994, 2000) simulated the Chinese 0.05° × 0.05° gridded long-term mean climatology based on 2450 station mean

values for monthly temperature, monthly percentage of potential sunshine hours, and monthly total precipitation throughout China and its adjacent regions. An atmospheric CO_2 concentration of 340 ppmv was used to link BIOME4 to the present-day baseline simulation.

Biomes	Plant functional types
Sub-tropical broad-leaved forest	Tropical broad-leaved evergreen Tropical broad-leaved raingreen Temperate broad-leaved evergreen
Montane broad-leaved forest	Temperate broad-leaved evergreen Temperate broad-leaved summergreen
Sub-alpine coniferous-leaf forest	Temperate coniferous-leaf evergreen Temperate summergreen conifer Boreal coniferous-leaf evergreen
Montane shrub steppe	Temperate xerophytic shrub Temperate grass
Montane steppe	Temperate grass Temperate xerophytic shrub
Alpine meadow	Cold graminoid or forb Cushion forb
Alpine steppe	Cold graminoid or forb Cold shrub
Montane desert	Cold shrub Cold graminoid or forb
Alpine desert	Cold shrub Cold graminoid or forb
Deciduous coniferous broad–leaf forest	Temperate broad-leaved summergreen Temperate coniferous-leaf evergreen Temperate summergreen conifer

Table 7. Biomes and plant functional types on the Tibetan Plateau at present

4.2.2 Future climate projection

The climatic conditions under increasing greenhousegas concentrations and sulfate aerosols have been simulated by atmospheric general circulation models (AGCMs). These models were commonly used in the construction and application of climate change scenarios for climate change impacts assessments (Neilson et al., 1998; Cramer et al., 2001). HadCM3 is a coupled atmosphere-ocean GCM developed at the Hadley Centre (Cox et al., 1999). The model was driven by computing the averages for 1931-1960 and for 2070-2099. We used the mean climate anomalies, and then interpolated the anomalies to the grid in high resolution (Fig. 9).

The anomalies were added to the baseline climatology to produce the climate fields used to drive improved BIOME4 to assess the sensitivity of alpine vegetation to possible future climate changes. The emissions scenario (Anon., 1996) included an increase in atmospheric CO_2 concentration from 340 to 500 ppmv and increase in sulphate aerosol concentration for the 21st century simulation. The simulation is not intended as a realistic forward projection and it was used to illustrate a possible course of climate change and thus to give an impression of the sensitivity of alpine ecosystems to climate change.

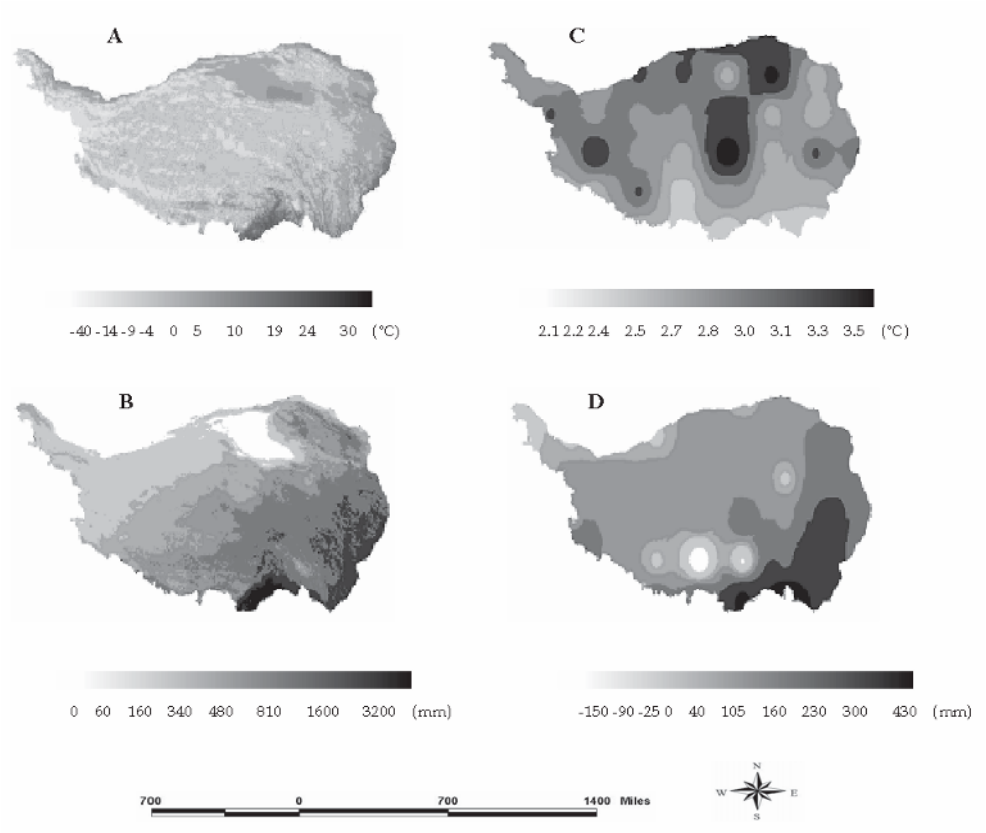

Fig. 9. Annual mean temperature (**A**) and annual precipitation (**B**) on the Tibetan Plateau, and anomalies in annual mean temperature (**C**) and annual precipitation (**D**) simulated by the Hadley Centre GCM (Johns et al., 1997; Mitchell et al., 1995).

4.2.3 Soil data

A digitized soil texture data set for the Tibetan Plateau was derived from Xiong & Li (1987). The soil texture information was interpolated to 0.05° × 0.05° grid cells. Eight soil types were classified.

4.2.4 Vegetation data

A map of potential natural vegetation of the Tibetan Plateau on 0.05° × 0.05° grid cells was derived from a digital vegetation map at a scale of 1 : 4 000 000 (Hou et al., 1982), which presents 113 vegetation units. These units were classified into nine categories based on the physical-geographical regions system of the Tibetan Plateau (Zheng, 1996). Each vegetation type was required to be floristically distinguishable to compare them with simulated vegetation maps (Fig. 10a, b).

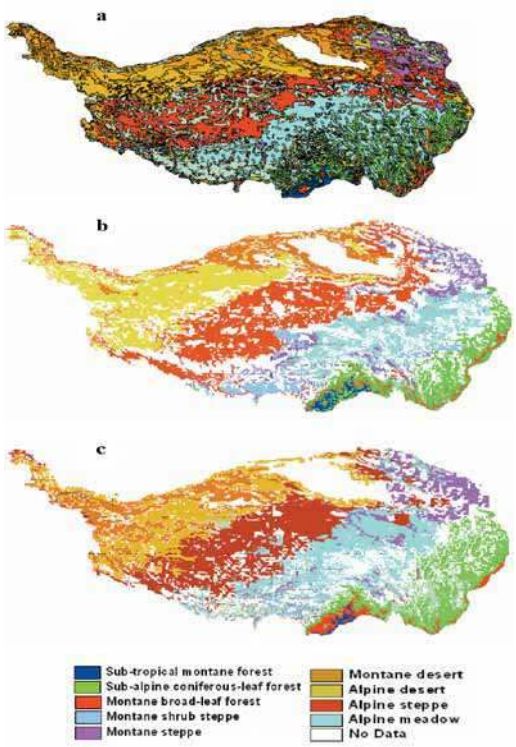

Fig. 10. Biomes on the Tibetan Plateau
a. Natural vegetation patterns
b. Biomes simulated by improved BIOME4
c. Biomes predicted by improved BIOME4

4.2.5 Assessment of the simulated results

The agreement between simulated and natural vegetation maps or reconstructed vegetation maps was quantified by the ΔV value. ΔV is a nontrivial and attribute-based measure of dissimilarity between biomes (Sykes et al., 1999). Dissimilarity between two maps (ΔV) was obtained by area-weighted averaging of ΔV over the model grid. The criterion of ΔV was cited (Sykes et al., 1999). ΔV values < 0.15 can be considered to point to excellent agreement between simulated and actual distributions, 0.15-0.30 is very good, 0.30-0.45 good, 0.45-0.60 fair, 0.60-0.80 poor, and > 0.80 very poor.

4.3 Results and discussions

4.3.1 Present day

In a quantitative comparison between the simulated vegetation map and the modern natural vegetation map, 80.1% of grid cells (80100 cells) showed the same biome (Fig. 10). Percentage agreement for grid cells assigned to specific biomes in the natural vegetation map were: sub-tropical montane forest 65.4%; sub-alpine coniferous forest 50.5%; montane broad-leaved forest 49.7%; montane shrub steppe 43.6%; montane steppe 55.0%; montane desert 77.9%; alpine desert 81.3%; alpine steppe 85.1%; alpine meadow 68.5%. The ΔV values

of each biome suggest that it is in excellent agreement for montane broad-leaved forest, sub-alpine coniferous forest and montane desert, and very good agreement for sub-tropical montane forest and alpine desert, and a good agreement for montane steppe, and fair agreement for alpine meadow and alpine steppe, and poor agreement for montane shrub steppe (Table 8 and Fig. 10a,b).

Biome	Area (×1000 km²)		ΔV	
	A	B	C	D
Sub-tropical montane forest	86.09	79.91	0.21	0.65
Montane broad-leaved forest	200.13	210.93	0.13	0.27
Sub-alpine coniferous-leaf forest	320.05	332.16	0.14	0.33
Montane shrub steppe	120.91	130.42	0.61	0.67
Alpine meadow	263.10	194.09	0.55	0.58
Montane steppe	158.11	296.13	0.37	0.81
Alpine steppe	675.98	583.52	0.52	0.41
Montane desert	373.39	449.25	0.14	0.22
Alpine desert	244.96	169.64	0.22	0.39
No data (Lake)	79.24	75.91		
Total	2521.96	2521.96	0.32	0.51

Table 8. Area (× 1000 km²) and ΔV values for each biome of the Tibetan Plateau. A = areas of simulated biomes under the current climate with CO_2 concentration = 340 ppmv; B = areas of simulated biomes under a scenario at the end of the next century with CO_2 concentration = 500 ppmv; C = ΔV values for comparison between simulated biome under current climate and actual vegetation distribution; D = ΔV values for comparison between simulated biome under a scenario with CO_2 concentration of 500 ppmv and simulated biome under current climate with CO_2 concentration of 340 ppmv.

4.3.2 Sensitivity to future changes

In the illustrative simulation of a 'greenhouse climate', the potentially forested area of the Tibetan Plateau increased substantially (Fig. 10c). The area of sub-tropical montane forest is slightly reduced, with replacement by montane broad-leaved and sub-alpine coniferous forest. The simulated tree line is farther north in most sectors than at present. Trees potentially invade shrubland/ meadow types where only fragments of forest exist today. Thus the simulations indicate a great sensitivity of the forest limit to CO_2-induced warming (Lloyd & Rupp et al., 2003; Lloyd & Fastie, 2003). The 'greenhouse climate' simulation also indicates major northward shifts of the alpine meadow biomes and a future reduction in the areas occupied by shrub-dominated montane steppe. The boundary between montane desert and alpine desert is found farther south than today. Our model results indicate that the extension of alpine desert would be reduced, while the area of montane desert would increase under the future climate scenarios with an atmospheric CO_2 concentration of 500 ppmv (Fig. 10c).

The improved BIOME4 model captures the main features of vegetation distribution on the Tibetan Plateau, such as the position of the alpine forest limit, its species composition in vegetation, regional differentiation in vertical vegetation, and the extent of alpine meadow, alpine steppe, and alpine desert. The spatial differentiation of physical-geographical regions

on the plateau is determined mainly by topographic configuration and atmospheric circulation. The climate is warm and humid in the southeast, and cold and arid in the northwest (Zheng, 1996). The reduction in temperature and precipitation toward the northwest is the most important reason for the simplification of species complexity in the vegetation (Zhang et al., 1996). The vegetation types in this region change gradually from marine humid montane (tropical seasonal and rain forest, warm-temperate broad leaved evergreen forest, temperate deciduous forest, and conifer forest) in the southeastern region to continental semi-arid montane (temperate shrubland/meadow, temperate steppe, alpine meadow/shrubland, and alpine steppe) in the middle region to continental arid montainous (temperate desert, alpine desert, and ice/polar desert) in the north- western region (Ni, 2000).

The improved BIOME4 model simulated the biome distribution with very good agreement for the central and northwestern regions of the Tibetan Plateau (DV = 0.26 for non-forests), and with a good agreement for the southeast (ΔV = 0.32 for forests). Altogether 13.8% of the forest cells were simulated as non-forest due to misclassification, i.e. cold needle-leaved evergreen or cold deciduous forest cells were simulated as low and high shrub meadow, and 7.1% of non-forest cells were simulated as forest due to low and high shrub meadow cells being simulated as the tree-line forming biome. Under the control of both climate and complex physiognomy, the actual vegetation pattern on the Tibetan Plateau is a mosaic, especially for forest types in flat regions (Anon., 1980). But in our simulation, the model produced vegetation types with continuous distribution leading to unrealistic patterns. The major mismatches (where > 20% of cells assigned to one biome in the natural vegetation map were assigned to a different biome in the simulation) were between adjacent biomes in climate space (Fig. 10a, b). The simulated boundary between alpine meadow and alpine steppe is somewhat too far south. The natural vegetation map shows the boundary between alpine steppe and alpine desert farther northwest than the simulation, apparently because of lower temperature and humidity. Our model results cannot distinguish ice/polar desert from alpine desert (Fig. 10a, b). Vegetation patterns simulated by improved BIOME4 are similar to those modelled by Ni (2000) using BIOME3-China. In our simulation, shrubland and meadow were distinguished using additional PFTs specifically occurring in alpine vegetation (cold shrub, cold graminoid or forb, and cushion forb). Therefore, areas of montane steppe and alpine meadow simulated by improved BIOME4 are more precise.

In the simulation of future developments triggered by increased atmospheric CO_2 concentration both winter and summer temperatures rise throughout the region (Fig. 9). Simulated temperature anomalies in winter are generally higher than in summer. This trend can be confirmed by the climate change on the Tibetan Plateau during recent years, i.e. from 1951 to 1990 (Tang et al., 1998). Thus the CO_2 increase causes a large, year-round warming which produces a stronger effect on vegetation shifts. For example, there would be a reduction in sub-tropical montane forest, alpine meadow, alpine steppe and alpine desert, and an extension of montane broad-leaved forest, sub-alpine coniferous forest, montane shrub steppe, montane steppe and montane desert. These results are consistent with other reports that suggest a northward shift of the vegetation on the Tibetan Plateau under a warming climate (Ni, 2000; Zheng, 1996; Zhang et al., 1996).

5. Acknowledgments

We thank all these people Dr. Preminda Jacob and Chen Bo for assistance in the field at Haibei Alpine Meadow Ecosystem Station; Dr. Suzana Dragicevic, Verda Kocabas, and the

Simon Fraser University Spatial Information Systems (SIS) lab for their support of this research project; Dr. Jian Ni for his help from Max-Planck Institute for Biogeochemistry, Jena, Germany. Research was supported by Haibei Alpine Meadow Ecosystem Station 90-0318, the Biosphere Program, U. S. State Department Grant 1753-900561, and in part by U.S. International Tundra Experiment (USITEX)(NSF/OPP-9321730), and was financially supported in part by The Key Project funded by the Chinese Academy of Sciences (KZCX3-SW-339), and The National Natural Science Foundation (40331066). We thank all these exports who participated in these projects, Prof. XingMin Zhou, Dr. Richard Cincotta, Dr. CaiPing Zhou, Prof. Hua Ouyang, Dr. Mechael Peterman, Dr. Dorin Aun, Prof. YanMing Zhang, and Dr. Andy Parson.

6. References

Anon. (The scientific expedition teams to the Tibetan Plateau, Chinese Academy of Sciences) (1980). *Vegetation of Tibet*. Science Press, Beijing, CN. (In Chinese.)

Anon. (The scientific expedition teams to the Tibetan Plateau, Chinese Academy of Sciences) (1985). *Forests of Xizang*. Science Press, Beijing, CN. (In Chinese.)

Anon. (Intergovernmental panel on climate change working group I). 1996. *Climate change 1995: The science of climate change*. Cambridge University Press, New York, NY, US.

Billings, W. D. (1987). Constraints to plant growth, reproduction and establishment in arctic environments. Arctic and Alpine Research, 19: 357-365.

Black, R. A., Richards, J. R., & Manwaring, J. H. (1994). Nutrient uptake from enriched microsites by three Great Basin perennials. *Ecology* 75: 110-122.

Bowman, W. D., Theodose, T. A., Schardt, J. C., & Conant, R. T. (1993). Constraints of nutrient availability on primary production in two alpine tundra community. *Ecology* 74: 2085-2097.

Briske, D. D. & Butler, J. L., (1989). Density-dependent regulation of ramet populations within the bunchgrass Schizachyrium scoparium: interclonal versus intraclonal interence. *Journal of Ecology* 77: 963-974.

Brooks, P. D., Williams, M. W., Walker, D. A., & Schmidt, S. K. (1995). The Niwot Ridge snow fence experiment: Biogeo-chemical responses to changes in the seasonal snowpack. In Tonnessen, K., Williams, M. W., and Tanter, M. (eds.), *Biogeochemistry of Seasonally Snow-Covered Catchments (Proceedings of a Boulder Symposium, July 1995)*. International Association of Hydrological Sciences Publication 228, 293-302.

Cao, M.K & Woodward, F.I. (1998). Net primary and ecosytem production and carbon stocks of terrestrial ecosytems and their responses to climate cxhange. *Global Change Biology*, 4:185-198.

Chapin, F S. & Shaver, G. R. (1985). Individualistic growth response of tundra plant species to environmental manipulations in the field. *Ecology* 66: 564-576.

Chapin, F S., Jefferies, R. L., Reynolds, J. E, and Svoboda, J., 1992: Arctic plant physiological ecology in an ecosystem context. In Chapin, E S., Jefferies, R. L., Reynolds, J. E, Shaver, G. R., & Svoboda, J. (eds), *Arctic Ecosystems in a Changing Climate: An Ecophysiological Perspective*. San Diego: Academic Press, 441-452.

Chapin, F. S., Shaver, G. R., Giblin, A. E., Nadeloffer, K. J., & Laundre, J. A. (1995). Responses of arctic tundra to experimental and observed changes in climate. *Ecology* 76: 694-711.

Chapin, F.S. III, Walker, B.H., Hobbs, R.J., Hooper, D,U., Lawton, J.H.,Sala, O.E. & Tilman, D., (1997). Biotic control over the functioning of Ecosytsem. Science. 277.5325: 500-504.

Chapin, F. S., III, McGuire, A. D., Randerson, J., Pielke, R. Sr, Baldocchi, D., Hobbie, S. E., Roulet, N., Eugster, W., Kasischke, E., Rastetter, E. B., Zimov, S. A., & Running, S. W. (2000). Arctic and boreal ecosystems of western North America as components of the climate system. *Global Change Biology* 6: 211–223.

Chapin, F. S., III, Robards, M. D., Huntington, H. P., Johnstone, J. F., Trainor, S. F., Kofinas, G. P., Ruess, R. W., Fresco, N., Natcher, D. C. & Naylor, R. L. (2006). Directional changes in ecological communities and social-ecological systems: a framework for prediction based on Alaskan examples. *The American Naturalist* 168: S36–S49.

Cincotta, R. P., Zhang, Y. Q., & Zhou, X. M. (1992). Transhumant alpine pastoralism in northwestern Qinghaip rovince: An evaluation of livestock population response during China's agrarian economic reform. *Nomadic People* 30: 3-25.

Coulelis, H. (1985). Cellular world: a framework for modeling micro-macro dynamics. *Environment and Planning* A 17: 585–596.

Cox, P., Betts, R., Bunton, C., Essery, R., Rowntree, P.R. & Smith, J. (1999). The impact of new land surface physics on the GCM simulation of climate and climate sensitivity. *Clim. Dynamics* 15: 183-203.

Cramer, W. & Leemans, R. (1991). Assessing impacts of climate change on vegetation using climate classification systems. In: Shugart, H.H. & Solomon, A.M. (eds.) *Vegetation dynamics and global change*, pp. 190-217. Chapman & Hall, New York, NY, US.

Cramer W., Bondeau A., Woodward F. I., Prentice I. C., Betts R. A., Brovkin V., Cox P., Fisher V., Foley J. A., F riend A. D., Kucharikch C., Lomas M. R., R amankutty N., Sitch S., Smith B., White A. & Molling C.Y. (2001). Global response of terrestrial ecosystem structure and function to CO2 and climate change: results from six dynamic global vegetation models. *Global Change Biol.* 7: 357-373.

Daly, C., Neilson, R.P. & Phillips, D.L. (1994). A statistical-topographic model for mapping climatological precipitation over mountainous terrain. *J Appl. Meteorol*. 33: 140-158.

Daly, C., Gibson, W.P., Hannaway, D. & Taylor, G.H. (2000). Development of new climate and plant adaptation maps for China. In: *Proceedings of the 12th Conference on Applied Climatology, May 8-11, 2000*. American Meteorogical Society, Asheville, NC, US.

Eastman, J. R. (2003). *IDRISI Kilimanjaro Tutorial. Manual Version 14.0*. Worcester, Massachusetts: Clark Labs of Clark University, 61–123.

Falkengren-Grerup, U . (1995). Interspecies differences in the preference of ammonium and nitrate in vascular plants. *Oecologia* 102: 305-311.

Giles, J. (2002). What kind of science is this? *Nature* 417: 216–218.

Grabherr. G., Gottfried,M . & Pauli, H. (1994). Climate effects on mountain plants. *Nature* 369: 448-450.

Harrison, S.P. & Prentice, I.C. (2003). Climate and CO2 controls on global vegetation distribution at the last glacial maximum: analysis based on palaeovegetation data, biome modellingand palaeoclimate simulations. *Global Change Biology* 9: 983-989.

Haxeltine, A. & Prentice, I.C. (1996). BIOME3: an equilibrium terrestrial biosphere model based on ecophysiological constraints, resource availability and competition among plant functional types. *Global Biogeochem. Cycl*. 10: 693-709.

Hodkinson, I. D., Webb, N. R., Bale, J. S. & Block, W. (1999). Hydrology, water availability and tundra ecosystem function in a changing climate: the need for a closer integration of ideas? *Global Change Biology* 5(3): 359–369.

Hou, X.Y., Sun, S.Z., Zhang, J.W., He, M.G., Wang, Y.F., Kong, D.Z. & Wang, S.Q. (1982). *Vegetation map of the people's Republic of China. Map Press of China*, Beijing, CN.

Itami, R. M. (1994). Simulating spatial dynamics: cellular automata theory. *Landscape and Urban Planning* 30: 27–47.

Jackson, L. E., Schimel, J. P. & Firestone, M. K. (1989). Short-term partitioning of ammonium and nitrate between plants and microbes in an annual grassland. *Soil Biology and Biochemistry* 21: 409-415.

Johnes, P. D. & Briffa, K. R. (1992). Global surface air temperature variations during the twentieth century. Part I: spatial, temporal and seasonal details. *The Holocene* 2: 165–179.

Jonasson, S., Havstrom, M., Jensen, M. & Callaghan, T. V. (1993). In situ mineralization of nitrogen and phosphorus of arctic soils afterp erturbations imulatingc limate change. *Oecologia* 95: 179-186.

Kaplan, J.O., Bigelow, N.H., Prentice, I.C., Harrison, S.P., Bartlein, J., Christensen, T.R., Cramer, W., Matveyeva, N.V., McGuire, A.D., Murray, D.F., Razzhivin, V.Y., Smith, B., Walker, D.A., Anderson, P.M., Andreev, A.A., Brubaker, L.B., Edwards, M.E. & Lozhkin, A.V. (2003). Climate change and Arctic ecosystems: 2. Modeling, paleodata model comparison and future projections. J. *Geophys. Res*. 108 (D19):8171.

Karlsson, P. S. (1985). Effect of water and mineral nutrient supply on a deciduous and evergreen dwarf shrub: Vaccinium uliginosum L. and V. vitisidaea L. Holarctic. *Ecology* 8: 1-8.

Kato, T., Tang, Y., Gu, S.,Hirota, M., Du,M., Li, Y. & Zhao, X. (2006). Temperature and biomass influences on interannual changes in CO2 exchange in an alpine meadow on the Qinghai-Tibetan Plateau. *Global Change Biology* 12:1285-1298.

Kennedy, A. D. (1995), Simulated climate change: are passive greenhouse a valid microcosn for testing the biological effects of environmental perturbation? *Global Change Biology* 1: 29-42.

Klanderud, K. & Birks, H.J.B. (2003). Recent increases in species richness and shifts in altitudinal distributions of Norwegian mountain plants. *Holocene* 13: 1-6.

Klein, J.A., Harte J. & Zhao X.Q. (2007). Experimental warming, not grazing, decreases rangeland quality on the Tibetian Plateau. *Ecological Applications* 17(2):341-557.

Korner, Ch. (1992). Response of alpine vegetation to global climate change. *In: International Conference on Landscape Ecological Impact of Climate Change*. Lunteren, The Netherlands, Catena Verlag, Supplement, 22: 85-96.

Leemans, R.E. (2004). Anotherreason for concern: regional and global impacts on ecosytems for different levels of climate change. *Global Environmental Change* 14: 219–228.

Li, Y. N., Zhao, X. Q., Cao, G. M., Zhao, L. & Wang, Q. X. (2004). Analysis on climates and vegetation productivity background at Haibei Alpine Meadow Ecosystem Research Station. *Plateau* Meteorology 23(4): 558–567.

Li, X., Cheng, G. D. & Lu, L. (2005). Spatial analysis of air temperature in the Qinghai-Tibet Plateau. *Arctic, Antarctic, and Alpine Researc*h 37(2): 246–252.

Lloyd, A.H., T. S. Rupp, C.L. Fastie & A. M. Starfield. (2003). Patterns and dynamics of treeline advance on the Seward Peninsula, Alaska. *Journal of Geophysical Research Atmospheres*. 108 (D2): 8161, doi: 10.1029/2001JD000852.

Lloyd, A.H. & C.L. Fastie (2003). Recent changes in treeline forest distribution and structure in interior Alaska. *Ecoscience*. 10(2):176-185.

Maxwell, B., (1992). Arctic climate: Potential for change under global warming. In Chapin, F S., Jefferies, R. L., Reynolds, J. F, Shaver, G. R., and Svoboda, J. (eds), *Arctic Ecosystems in a Changing Climate: An Ecophysiological Perspective*. San Diego: Academic Press, 11-34.

McGuire, A. D., Chapin, F. S., III, Walsh, J. E. & Wirth, C. (2006). Integrated regional changes in arctic climate feedbacks: implications for the global climate system. *Annual Review of Environmental* Resources 31: 61–91.

Molau, U. & Alatalo, J.M. (1998). Responses of subarctic alpine plant communities to simulated environmental change: Biodiversity of bryophytes, lichens, and vascular plants. *Ambio* 27: 322-329.

Murry, C. & Miller, P. C. (1982). Phenological observations of major plant growth forms and species in montane and Eriophorum vaginatum tussock tundra in central Alaska. *Holarctic Ecology* 5: 109-116.

Nadelhoffer, K. J., Giblin, A. E., Shaver, G. R. & Laundre, J. A. (1991). Effects of temperature and substrate quality on element mineralization in six arctic soils. *Ecology* 72: 242-253.

Neilson, R., Prentice, I.C. & Smith, B. (1998). Simulated changes in vegetation distribution under global warming. In: Watson, R.T. et al. (eds.) *The regional impacts of climate change*, pp. 439-456. Cambridge University Press, New York, NY, US.

Ni, J. (2000). A simulation of biomes on the Tibetan Plateau and their responses to global climate change. *Mou*nt. *Res. Devel.* 20: 80-89.

Parmesan, C. (1996). Climate and species' range. *Nature* 382: 765-766.

Parmesan, C., Ryholm, N., Stefanescu, C., Hill, J. K. et al. (1999). Poleward shifts in geographical ranges of butterfly species associated with regional warming. *Nature* 399: 579-583.

Parsons, A. N., Welker, J. M., Wookey, P. A., Press, M. C., Callaghan, T. V. & Lee, J. A. (1994). Growth responses of four sub-arctic dwarf shrubs to simulated climate change. *Journal of Ecology*, 82: 307-318.

Parsons, A. N., Press, M. C., Wookey, P. A., Welker, J. M., Robinson, C. H., Callaghan T. V. & Lee, J. A. (1995). Growth and reproductive output of Calamagrostis lapponica in response to simulated environmental change in the subarctic. *Oikos* 72:61-66.

Pauli, H., Gottfried, M. & Grabherr, G. (2003). The Piz Linard (3411m), the Grisons, Switzerland – Europe's oldest mountain vegetation study site. In: Nagy, L., Grabherr, G., Körner, C. & Thompson, D.B.A. (eds.) *Alpine biodiversity in Europe – A Europe-wide assessment of biological richness and change*, pp. 443-448. Springer-Verlag, Berlin, DE.

Robinson, C. H., Wookey, P. A., Parsons, A. N., Potter, J. A., Callaghan, T. V., Lee, J. A., Press, M. C. & Welker, J. M. (1995). Responses of plant litter decomposition and nitrogen mineralisation to simulated environmental change in a high arctic polar semi-desert and a subarctic dwarf shrub heath. *Oikos*, 74: 503-512.

Rozanski, K., Araguas-Araguas, L. & Gonfiantini,R. (1992). Relation between long-term trends of oxygen-18 isotope composition of precipitation and climate. *Science* 258: 981-985.

Ruxton, G. D., and Saravia, L. A. (1998). The need for biological realism in the updating of cellular automata models. *Ecological Modelin*g 107(2–3): 105–112.

Sala, O. E., and Lauenroth, W. K. and Parton, W. J. (1992). Long-term soil water dynamics in the shortgrass steppe. *Ecology* 73: 1175-1181.

Schimel, J. S., Bilbrough, C. B. and Welker, J. M. 2004. The effect of changing snow cover on yearround soil nitrogen dynamics in Arctic tundra ecosystems. *Soil Biology and Biochemistry* 36: 217-227.

Shaver, G. R., Billings, W. D., Chapin, E S., Giblin, A. E., Na-delhoffer, K. J., Oechel, W. C. & Rastetter, E. B. (1992). Global change and the carbon balance of arctic ecosystems. *Bioscience* 42: 433-441.

Shaver, G. R. & Chapin, E S. (1991). Production:biomass relationships and element cycling in contrasting arctic vegetation types. *Ecological Monographs* 61: 1-31.

Song, M., Zhou, C. & Ouyang, H. (2005). Simulated distribution of vegetation types in response to climate chang on the Tibetan Plateau. *Journal of Vegetation Science* 16:341-350.

Sullivan, P. F. & Welker, J. M. 2005. Warming chambers stimulate early season growth of an arctic sedge: results of a minirhizotron field study. *Oecologia* 142: 616-626.

Sykes, M.T., Prentice, I.C. & Laarlf, F. (1999). Quantifying the impact of global climate change on potential natural vegetation. *Clim. Change* 41: 37-52.

Tang, M.C., Cheng, G.D. & Lin, Z.Y. (1998*). Contemporary climatic variations over Tibetan Plateau and their influences on environments*. Guangdong Science & Technology Press, Guangzhou, CN.

Tape, K., Sturm, M. & Racine, C. (2006). The evidence for shrub expansion in Northern Alaska and the Pan-Arctic. *Global Change Biol.* 12, 686–702.

Thompson, L., G., Mosley-Thompson, E., Bolzan, J. F. et al. (1989). Holocene-Late Pleistocene climatic ice core records from Qinghai-Tibetan Plateau. *Science* 246: 474-477.

Walker, M. D., Webber, P. J., Arnold, E. H. & Ebert-May, D. (1994). Effects of interannual climate variation on aboveground phytomass in alpine vegetation. *Ecology* 75:393-408.

Walther, G.R., Post, E., Convey, P., Menzel, A., Parmesan, C., Beebee, T.J.C., Fromentin, J.M., Hoegh-Guldberg, O. & Bairlein, F. (2002). Ecology responses to recent climate change. *Nature* 416: 389-395.

Welker, J. M., Rykiel, E. J., Briske, D. D. & Goeschel, J. D. (1985). Carbon import among vegetative tillers within two bunchgrasses: assessment with carbon-11 labelling. *Oecologia* 67: 209-212.

Welker, J. M., Briske, D. D. & Weaver, R. W. (1987). Nitrogen-15 partitioning within a three generation tiller sequence of the bunchgras Schizachyrium scoparium: response to selective defoliation. *Oecologia* 74: 330-334.

Welker, J. M. & Briske, D. D. (1992). Clonal biology of the temperate caespitose graminoid Schizachyrium scoparium: A synthesis with reference to climate change. *Oikos* 56:357- 365.

Welker, J. M., Wookey, P., Parsons, A. P., Callaghan, T. V., Press, M. C. & Lee, J. A. (1993). Leaf carbon isotope discrimination and demographic responses of Dryas octopetala

to water and temperature manipulations in a high arctic polar semi-desert, Svalbard. *Oeclogia* 95: 463-749.

Welker, J. M., Svoboda, J., Henry, G., Molau, U., Parsons, A. N. & Wookey, P. A. (1995). Response of two Dryas species to ITEX environmental manipulations: A synthesis with circumpolar comparisions. In: *Proceedings from the 6th International Tundra Experiment (ITEX)*. Ottawa, Canada. April 1995. Abstract.

Welker, J. M., Fahnestock, J. T. & Jones, M. H. 2000. Annual CO2 flux from dry and moist arctic tundra: field responses to increases in summer temperature and winter snow depth. Climatic Change 44: 139-150.

Welker, J.M., Fahnestock, J.T., Povirk, K., Bilbrough, C. & Piper, R. 2004. Carbon and nitrogen dynamics in a long-term grazed alpine grassland. *Arctic, Antarctic and Alpine Research* 36: 10-19.

Welker, J. M., Fahnestock, J. T., Sullivan, P. & Chimner, R. A. (2005). Leaf mineral nutrition of arctic plants in response to long-term warming and deeper snow in N. Alaska. *Oikos* 109: 167-177.

White, R. & Engelen, G. (2000). High-resolution integrated modeling of the spatial dynamics of urban and regional system. *Environment and Urban Systems* 24: 383–400.

Wolfram, S. (1984). Cellular automata as models of complexity. Nature 311(4): 419–424.

Woodward, F.I. 1987. *Climate and plant distribution*. Cambridge University Press, Cambridge, UK.

Wookey, P. A., Parsons, A. N., Welker, J. M., Potter, J., Callaghan, T. V., Lee, J. A. & Press, M. C. (1993). Comparative responses of phenology and reproductive development to sim-ulated environmental change in sub-arctic and high arctic plants. *Oikos* 67: 490-502.

Wookey, P. A., Welker, J. M., Parsons, A. N., Press, M. C., Callaghan, T. V. & Lee, J. A. (1994). Differential growth, allocation and photosynthetic responses of *Polygonum viviparum* to simulated environmental change at a high arctic polar semi-desert. Oikos 70: 131-139.

Wookey, P. A., Robinson, C. H., Parsons, A. N., Welker, J. M., Press, M. C., Callaghan, T. V. & Lee, J. A. (1995). Environmental constraints on the growth, photosynthesis and reproductive development of Dryas octopetala at a high arctic polar semi-desert, Svalbard. *Oecologia* 102: 478-489.

Xiong Y. & Li, Q.K. (1987). *Soils in China*. Science Press, Beijing.

Xia, W. P. (1988). A brief introduction to the fundamental characteristics and the work in Haibei Research Station of Alpine Meadow Ecosystem. Proceedings of the *International Symposium of an Alpine Meadow Ecosystem*. Bejing: Academic Sinica, 1-10.

Yu, G. (1999). Studies on biomization and the global palaeovegetation project. *Adv. Earth Sci.* 14: 306-311.

Yu, G., Sun, X.J., Qin, B.Q., Song, C.Q., Li, H.Y., Prentice, I.C. & Harrison, S.P. (1998). Pollenbased reconstruction of vegetation patterns of China in mid-Holocene. *Sci. China (Ser. D)* 41: 130-136.

Zhang, X.S. (1993). The Tibetan Plateau in relation to the vegetation of China. *Ann. Missouri Bot. Garden* 70: 564-570.

Zhang, X.S., Yang, D.A., Zhou, G.S., Liu, C.Y. & Zhang, J. (1996). Model expectation of impacts of global climate change on biomes of the Tibetan Plateau. In: Omasa, K.,

Kai, K., Taoda, H., Uchijima, Z. & Yoshino, M. (eds.) *Climate change and plants in East Asia* pp. 25-38. Springer-Verlag, Tokyo, JP.

Zhang, Y. M., and Liu, J. K. (2003). Effects of plateau zokors (Myospalax *fontanierii*) effects on plant community and soil in an alpine meadow. *Journal of Mammalogy* 84(2): 644–651.

Zhang, Y. Q. (1990). A quantitative study on the characteristics and succession pattern of alpine shrublands under the different grazing intensities. *Acta Phytoecologia and Geobotanica Sinica* 14(4): 358–365.

Zhang, Y. Q. & Zhou, X. M. (1992). The quantitative classification and ordination of Haibei alpine meadow. *Acta Phytoecological ET Geobotanica Sinica* 16(1): 36–42.

Zhang, Y. Q. & Welker, J. M. (1996). Tibetan alpine tundra responses to simulated changes in climate: aboveground biomass and community responses. *Arctic and Alpine Research* 28(2): 203–209.

Zhang, Y. Q. (2005). Raster multi-criteria evaluation for experimental design with aggregating weighed factors. *GeoTec Event Proceeding*. Poster Presentation in Vancouver Canada. (http:// www.sfu.ca/geog/geog355fall04/yqz/index.htm).

Zhang, Y.Q.A., Peterman, M.R.,Aun, D.L. & Zhang Y.M. (2008). Cellular Automata:Simulating alpine tundra vegetation dynamics in Response to global warming. *Arctic, Antarctic and Alpine Research* 40(1):256-263.

Zheng, D. (1996). The system of physico-geographical regions of the Tibet Plateau. *Sci. China (Ser. D)* 39: 410-417.

Zhou, X. M., Wang, Zh. B. & Du, Q. (1987). *Qinghai Vegetation*. Qinghai People Press.

Zhou, X.M. (2001). *Chinese kobresia meadows*. Science, Beijing.

Corresponding author: Yanqing A. Zhang, instca@yahoo.com

Global Warming

Edited by Stuart Arthur Harris

ISBN 978-953-307-149-7
Hard cover, 250 pages
Publisher Sciyo
Published online 27, September, 2010
Published in print edition September, 2010

This book is intended to introduce the reader to examples of the range of practical problems posed by "Global Warming". It includes 11 chapters split into 5 sections. Section 1 outlines the recent changes in the Indian Monsoon, the importance of greenhouse gases to life, and the relative importance of changes in solar radiation in causing the changes. Section 2 discusses the changes to natural hazards such as floods, retreating glaciers and potential sea level changes. Section 3 examines planning cities and transportation systems in the light of the changes, while section 4 looks at alternative energy sources. Section 5 estimates the changes to the carbon pool in the alpine meadows of the Qinghai-Tibet Plateau. The 11 authors come from 9 different countries, so the examples are taken from a truly international set of problems.

InTech Europe
University Campus STeP Ri
Slavka Krautzeka 83/A
51000 Rijeka, Croatia
Phone: +385 (51) 770 447
Fax: +385 (51) 686 166
www.intechopen.com

InTech China
Unit 405, Office Block, Hotel Equatorial Shanghai
No.65, Yan An Road (West), Shanghai, 200040, China
中国上海市延安西路65号上海国际贵都大饭店办公楼405单元
Phone: +86-21-62489820
Fax: +86-21-62489821